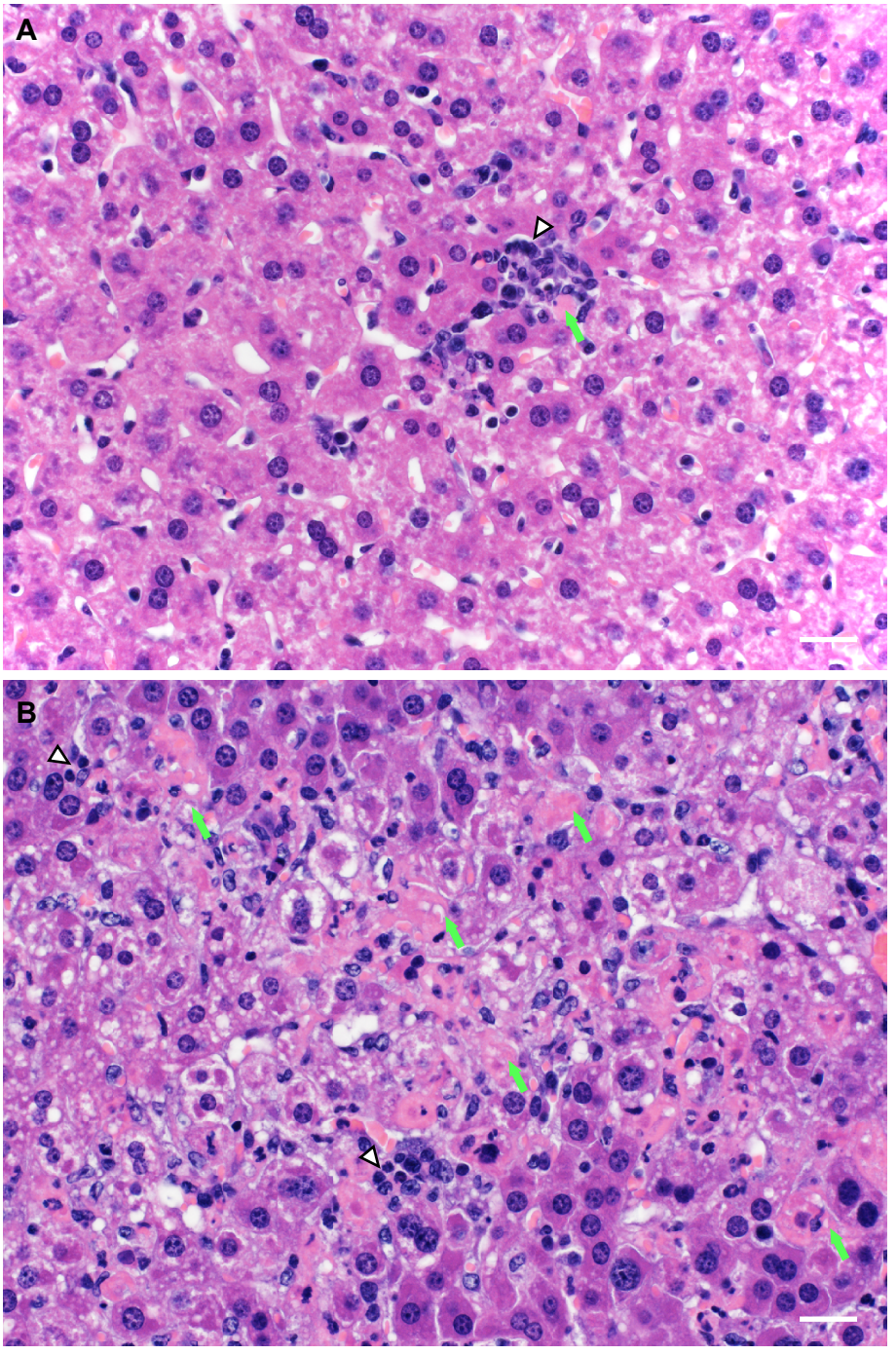

Figure S1: Pathologic changes in the liver at 5 dpi with MA-EBOV, Related to Figure 2. (A) C57Bl/6 mice had necrosis of individual hepatocytes (green arrow) that were bounded by infiltrates of small numbers on neutrophils and macrophages (white arrowhead). **(B)** MAVS$^{-/-}$ mice had large, coalescing foci of hepatocellular necrosis (green arrows) that were infiltrated by small to moderate numbers of neutrophils and macrophages (white arrowhead). Scale bar represents 20μm.

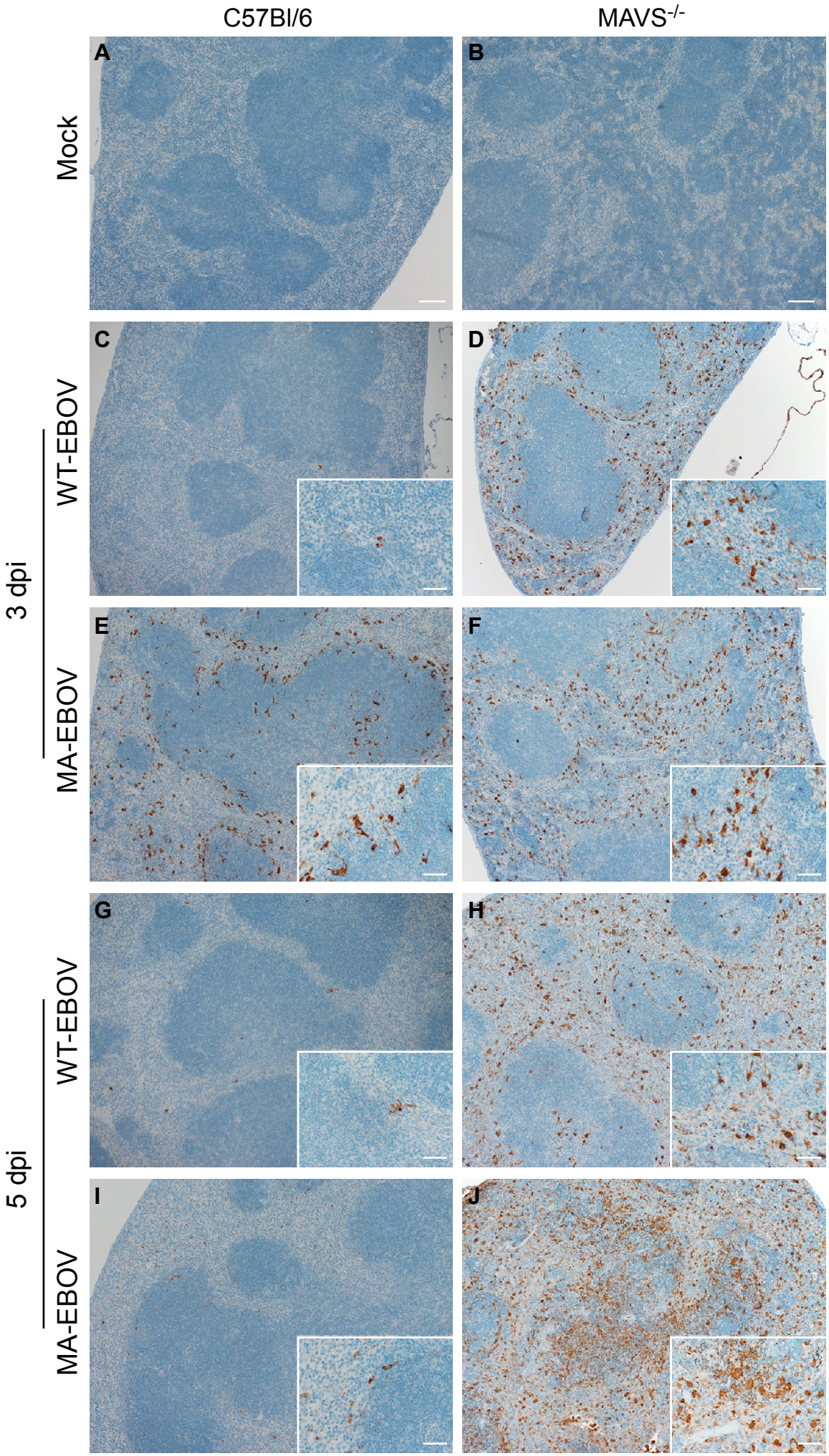
C57Bl/6
MAVS-/-
A
B
Mock
C
D
WT-EBOV
3 dpi
E
F
MA-EBOV
G
H
WT-EBOV
5 dpi
I
J
MA-EBOV

Figure S2: EBOV VP40 antigen in spleen of C57Bl/6 and MAVS$^{-/-}$ mice, Related to Figure 3. The presence of EBOV VP40 was examined by immunohistochemistry in C57Bl/6 or MAVS$^{-/-}$ mice that were **(A-B)** mock infected (scale bar =100μm), **(C-D)** infected with WT-EBOV at 3 dpi, **(E-F)** infected with MA-EBOV at 3 dpi, **(G-H)** infected with WT-EBOV at 5 dpi, or **(I-J)** infected with MA-EBOV at 3dpi. Insets (scale bar = 20μm) show greater detail of infected cells. In all conditions, macrophages and dendritic-like cells contain viral antigen. The absence of MAVS did not change cellular tropism of EBOV but did increase the numbers of infected cells in each tissue section.

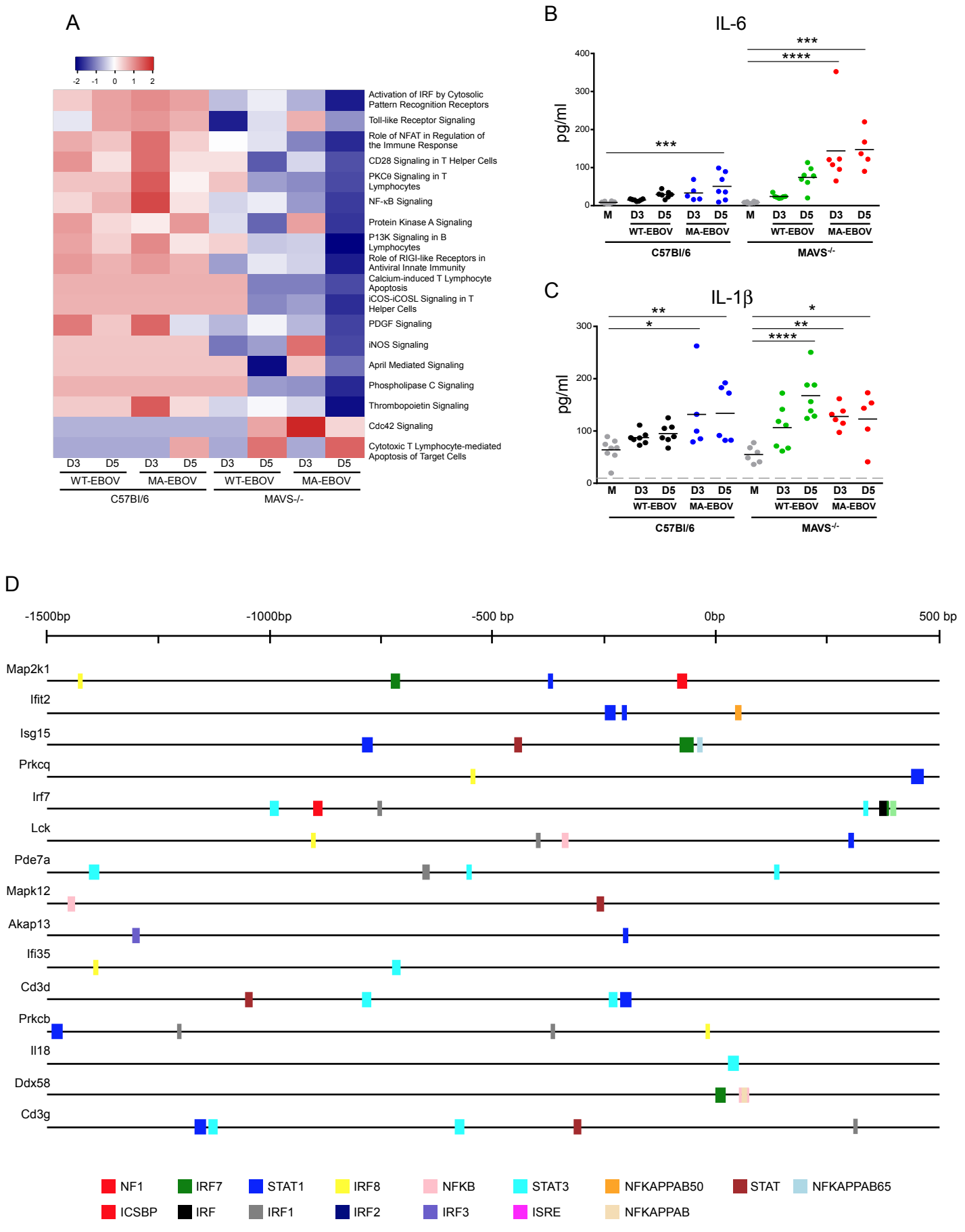
A
-2 -1 0 1 2
Activation of IRF by Cytosolic Pattern Recognition Receptors
Toll-like Receptor Signaling
Role of NFAT in Regulation of the Immune Response
CD28 Signaling in T Helper Cells
PKCθ Signaling in T Lymphocytes
NF-κB Signaling
Protein Kinase A Signaling
P13K Signaling in B Lymphocytes
Role of RIGI-like Receptors in Antiviral Innate Immunity
Calcium-induced T Lymphocyte Apoptosis
iCOS-iCOSL Signaling in T Helper Cells
PDGF Signaling
iNOS Signaling
April Mediated Signaling
Phospholipase C Signaling
Thrombopoietin Signaling
Cdc42 Signaling
Cytotoxic T Lymphocyte-mediated Apoptosis of Target Cells
D3 D5 D3 D5 D3 D5 D3 D5
WT-EBOV MA-EBOV WT-EBOV MA-EBOV
C57Bl/6 MAVS-/-
B
IL-6
pg/ml
400
300
200
100
0
***
***
****
M D3 D5 D3 D5 M D3 D5 D3 D5
WT-EBOV MA-EBOV WT-EBOV MA-EBOV
C57Bl/6 MAVS-/-
C
IL-1β
pg/ml
300
200
100
0
**
*
*
**
****
M D3 D5 D3 D5 M D3 D5 D3 D5
WT-EBOV MA-EBOV WT-EBOV MA-EBOV
C57Bl/6 MAVS-/-
D
-1500bp
-1000bp
-500 bp
0bp
500 bp
Map2k1
Ifit2
Isg15
Prkcq
Irf7
Lck
Pde7a
Mapk12
Akap13
Ifi35
Cd3d
Prkcb
Il18
Ddx58
Cd3g
NF1
IRF7
STAT1
IRF8
NFKB
STAT3
NFKAPPAB50
STAT
NFKAPPAB65
ICSBP
IRF
IRF1
IRF2
IRF3
ISRE
NFKAPPAB

Figure S3: Canonical pathway analysis of DEGs and promoter analysis for MAVS-independent DEGs, Related to Figure 4. (A) Comparative analysis of canonical pathways of DEG lists of spleen in all infection conditions (based on Fisher's exact test, performed with IPA software) were used to map pathways that showed significant difference between C57BL/6 and MAVS$^{-/-}$ mice (1.5 fold; P⩽0.01). **(B)** IL-6 or **(C)** IL-1 concentrations in the sera of EBOV-infected mice. *P<0.05, **P<0.01, ***P<0.001, ****P<0.0001 determined by one-way ANOVA with Dunnett's multiple comparison test. Data shown from two experiments with mean indicated by short black lines for each group; dashed line indicates limit of detection. **(D)** Sequence analysis of promoter regions from DEGs derived from spleen of WT-EBOV and MA-EBOV MAVS$^{-/-}$ mice.

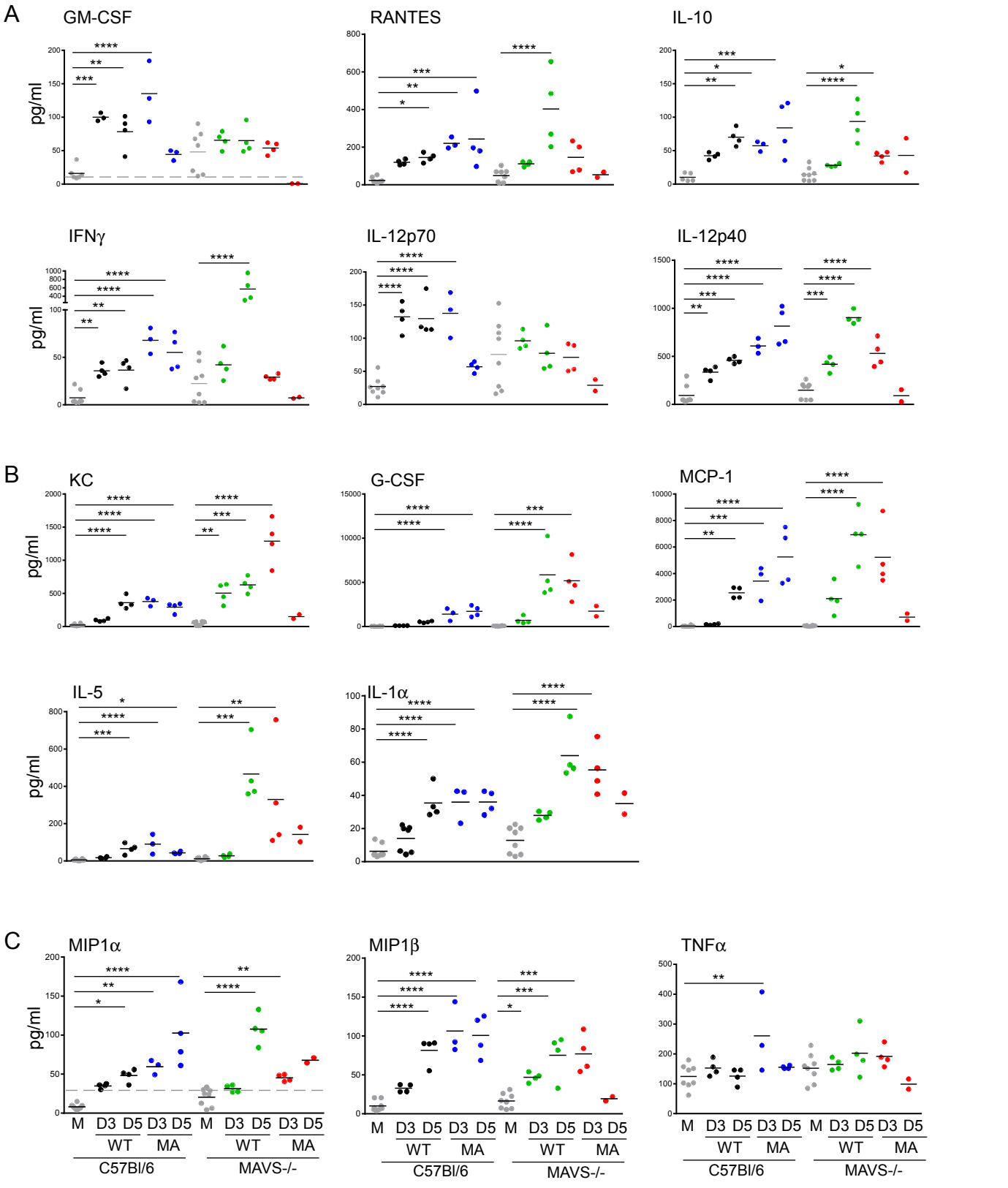

Figure S4: Serum cytokine expression following EBOV infection of C57Bl/6 and MAVS$^{-/-}$ mice, Related to Figure 5. Bio-plex analysis of serum cytokine expression shown as those cytokines associated with resistance to infection **(A)**, lethal infection **(B)**, or no clear relationship to disease **(C)**. Results are shown from one of two experiments performed. *P<0.05, **P<0.01, ***P<0.001, ****P<0.0001 determined by one-way ANOVA with Dunnett's multiple comparison test. Mean is indicated as short black lines for each group; dashed lines indicate limit of detection.

Supplemental Experimental Procedures

Viruses

MA-EBOV was originally derived from serial passage of Ebola virus strain Mayinga (species *Zaire ebolavirus*) in suckling BALB/c mice (Bray et al., 1998). MA-ZEBOV and WT-ZEBOV (Mayinga strain) were propagated in Vero E6 cells (African green monkey kidney cells) and the supernatants were collected to produce virus stocks. Infectivity of virus stocks was determined by a focus-forming assay on Vero E6 cells as previously described (Ebihara et al., 2006).

Neutralization of IFN-I and IFN-II responses in vivo

$MAVS^{-/-}$ mice were injected intraperitoneally (IP) (0.5 mg/dose in 0.5 ml PBS) with either anti-IFNAR1 (clone MAR1-5A3)(Sheehan et al., 2006), anti-IFN-γ (clone XMG1.2)(Cherwinski et al., 1987), both anti-IFNAR1 and anti-IFN-γ, or a rat IgG1 isotype control (clone RTK2071). All antibodies were ultra-LEAF purified from BioLegend.

Bone marrow-derived macrophages and quantitative RT-PCR

Bone marrow-derived macrophages (BMM) were differentiated in vitro from mouse bone marrow cells using macrophage colony-stimulating factor (M-CSF) as previously described (Griffin et al., 2013; Manzanero, 2012). Briefly, bone marrow cells were harvested from mouse femurs and cultured in complete DMEM (DMEM supplemented with 10% heat-inactivated fetal bovine serum (FBS, ThermoFisher), 2mM L-glutamine, 10mM HEPES, 0.1mM non-essential amino acids (NEAA, Gibco) 100U/ml penicillin and 100ug/ml streptomycin. Flow cytometry demonstrated >95% of cells expressed CD11b and F4/80 indicating high purity of bone marrow-derived macrophages. BMMs were seeded at $2\text{-}4 \times 10^5$ cells/well in a 24-well plate, and were stimulated with LPS (1 μg/ml, Invivogen), polyriboinosinic-polyribocytidylic acid (Poly I:C) (20 ng/ml, Invivogen), or infected with Sendai virus (200 units/well). Cells were collected at 5 hours and 18 hours following stimulation and total RNA was isolated using a Qiagen RNeasy Plus kit (Qiagen). For quantitative RT-PCR analysis, RNA was reverse transcribed using a SuperScript VILO cDNA synthesis kit (Life Technologies). cDNA was then used as a template in TaqMan-PCR reactions per manufacturer's instructions to quantify mRNA specific for IFNβ (assay ID: Mm00439546) and the housekeeping gene HPRT (assay ID: Mm01545399, Life Technologies). Reactions were analyzed using Applied Biosystems 7900HT real-time PCR system (Life Technologies). IFNβ mRNA was normalized to HPRT mRNA levels and expressed as fold change relative to RNA samples from unstimulated cells using the $2^{-\Delta\Delta Ct}$ method.

Flow cytometry

Fresh single cell preparations ($1\text{-}2 \times 10^6$ cells) were stained according to standard procedures. Briefly, cells were stained with a fixable Live/Dead cell viability reagent per manufacturer's instructions (Molecular Probes). Cells were then blocked with anti-mouse CD16/CD32 and stained with the following antibodies diluted in FACS wash buffer (PBS supplemented with 2% fetal calf serum and 2.5mM EDTA). CD3 (145-2C11), CD19 (1D3), CD11b (M1/70), CD11c (N418), Ly6C (HK1.4), F4/80 (BM8) (all purchased from eBiosciences) and Ly6G (1A8) (BD Biosciences).

For intracellular detection of MAVS, cells were fixed in 4% paraformaldehyde/PBS for 20 min at 4°C and permeabilized in 0.25% saponin/1%FBS/PBS. Intracellular staining was performed using a rodent specific MAVS antibody (Cell Signaling Technology) and Alexa 647-conjugated anti-rabbit IgG (Invitrogen). Multi-parameter data was acquired on a LSRII flow cytometer (BD) and analyzed using FlowJo software. Dead cells, debris and doublets were excluded from all analyses.

Leukocyte populations were defined as follows: T lymphocytes (CD11b-, CD11c-, CD19- and CD3+), B lymphocytes (CD11b-, CD11c-, CD19+ and CD3-), neutrophils (CD11b^{hi}, Ly6G+), monocytes (CD11b^{hi}, Ly6G-, Ly6C+), myeloid DC (CD19-, CD11b+, CD11c^{hi}) and macrophages (CD11c^{low}, CD11b^{hi}, F4/80+).

Cytokine analysis by Bio-Plex assay and Lumikine ELISA.

Sera were collected from mock- and EBOV-infected mice at 3 and 5 days post-infection and inactivated by using γ-irradiation (5 MRad) and removed from the maximum containment laboratory. Concentrations of IFNα and INFβ were determined using a bioluminescent-based ELISA per manufacturer's instructions (Invivogen). The IFNα ELISA detects multiple subtypes (IFN-α1, -α2, -α4, -α5 and -α6). Cytokine concentrations in serum were also measured using a mouse 23-cytokine Bio-Plex Pro Assay according to the manufacturer's instructions (BioRad).

RNA preparation and oligonucleotide microarray processing.

RNA was extracted from mouse spleens and livers using a Qiagen RNeasy Minikit with RNAlater solution (Qiagen, Valencia, CA) according to the manufacturer's instructions. RNA was further purified using RNeasy columns (Qiagen, Valencia, CA). RNA samples were spectroscopically verified for purity, and the quality of the intact RNA was assessed using an Agilent 2100 Bioanalyzer. For each set of treatment conditions, three of the five RNA samples exhibiting the highest RNA integrity number (RIN) determined using the Bioanalyzer were used for microarray analysis. cRNA probes were generated from each sample by the use of an Agilent one-color LowInput Quick Amp labeling kit (Agilent Technologies, Santa Clara, CA). Individual cRNA samples were hybridized to Agilent mouse whole-genome oligonucleotide 4-by-44 microarrays (approximately 39,000 unique mouse genes) according to the manufacturer's instructions. To enable examination of animal-to-animal variation as part of the data analysis, samples from individual animals were not pooled; included were samples from three animals per time point for each virus (60 animals total). Select samples were hybridized a second time (n = 2 technical replicates) to verify the quality of the process. Slides were scanned with an Agilent DNA microarray scanner, and the resulting images were analyzed using Agilent Feature Extractor version 8.1.1.1. This software was used to perform image analysis, including significance of signal and spatial detrending and to apply a universal error model. For these hybridizations, the most conservative error model was applied. Raw data were then loaded into a custom-designed laboratory information management system (LIMS). Data were warehoused in a Labkey system (Labkey, Inc., Seattle, WA) and analyzed as described below. Primary data are available in accordance with proposed Minimum Information About a Microarray Experiment (MIAME) standards through the Gene Expression Omnibus (GEO: GSE83309).

Microarray analysis and bioinformatics.

Global gene expression in infected spleens was compared to that in control RNA prepared from a pool of equal masses of total RNA from spleen tissue of five uninfected mice. Probe labeling and microarray slide hybridization were performed as described elsewhere (Forero et al., 2015).

Raw data from Agilent Feature Extractor was normalized by applying the central tendency algorithm with standard reference set at the 75th percentile of each microarray. Correlations between virus titers and gene expression were determined by Pearson's correlation coefficients. One- or two-way analysis of variance (ANOVA) was carried out for various groups of samples stratified by virus infection and/or time point (see Results for more grouping details). The primary transcriptomic data were extracted and "normalizeBetweenArrays" method available in the "limma" package of the R Bioconductor was used as previously described (Josset et al., 2012) to perform quantile normalization of the primary transcriptomic data. Furthermore the data was adjusted for batch effects using the ComBat software (Johnson et al., 2007). Using a linear model fit of the "limma" package, differential expressions were determined by comparing the average gene expression of EBOV infected replicates to the average of time-matched mock-infected samples. Criteria for differential expression were an absolute fold change cutoff of

1.5 and a p-value of ≤ 0.05 after adjustment using the Benjamini-Hochberg multiple testing correction. Additional clustering, creation of heatmaps, and other statistical analyses were all performed in R.

Functional and network analysis of statistically significant gene expression changes was performed using Ingenuity Pathways Analysis (IPA). The analysis considered all genes from statistical analysis results and those associated with biological functions in the IPA Knowledge Base. For all gene set enrichment analyses, Fisher's exact test was used to determine the probability that each biological function assigned to the genes within each statistical analysis result was due to chance alone. Additionally, significant canonical pathways identified from IPA were assigned a z-score which determines if gene expression changes from the expression data are consistent with the IPA Knowledge Base.

Histopathology and immunohistochemistry

Tissues were fixed in 10% Neutral Buffered Formalin x2 changes, for a minimum of 7 days. Tissues were placed in cassettes and processed with a Sakura VIP-6 Tissue Tek, on a 12 hour automated schedule, using a graded series of ethanol, xylene, and Ultraffin. Embedded tissues were sectioned at 5µm and dried overnight at 42ºC prior to staining. H&E staining was performed using standard methods. Tissue sections were read by a board-certified veterinary pathologist under blinded conditions.

Specific anti-Ebola immunoreactivity was detected using an Ebola Zaire VP40 polyclonal rabbit antibody at a 1:2000 dilution. Caspase 3 immunoreactivity was detected with anti-active caspase 3 antibody (Promega) at a 1:1200 dilution. Biotinylated anti-rabbit link (Biogenex) was used as the secondary antibody for both of the primaries listed above. The tissues were then processed for immunohistochemistry using the Discovery XT automated processor (Ventana Medical Systems) with a DABMap (Ventana Medical Systems) kit.

References:

Bray, M., Davis, K., Geisbert, T., Schmaljohn, C., and Huggins, J. (1998). A mouse model for evaluation of prophylaxis and therapy of Ebola hemorrhagic fever. J. Infect. Dis. *178*, 651-661.

Cherwinski, H.M., Schumacher, J.H., Brown, K.D., and Mosmann, T.R. (1987). Two types of mouse helper T cell clone. III. Further differences in lymphokine synthesis between Th1 and Th2 clones revealed by RNA hybridization, functionally monospecific bioassays, and monoclonal antibodies. J. Exp. Med. *166*, 1229-1244.

Ebihara, H., Takada, A., Kobasa, D., Jones, S., Neumann, G., Theriault, S., Bray, M., Feldmann, H., and Kawaoka, Y. (2006). Molecular determinants of Ebola virus virulence in mice. PLoS Pathog. *2*, e73.

Forero, A., Tisoncik-Go, J., Watanabe, T., Zhong, G., Hatta, M., Tchitchek, N., Selinger, C., Chang, J., Barker, K., Morrison, J., *et al.* (2015). The 1918 Influenza Virus PB2 Protein Enhances Virulence through the Disruption of Inflammatory and Wnt-Mediated Signaling in Mice. J. Virol. *90*, 2240-2253.

Griffin, A.J., Crane, D.D., Wehrly, T.D., Scott, D.P., and Bosio, C.M. (2013). Alternative activation of macrophages and induction of arginase are not components of pathogenesis mediated by Francisella species. PloS One *8*, e82096.

Johnson, W.E., Li, C., and Rabinovic, A. (2007). Adjusting batch effects in microarray expression data using empirical Bayes methods. Biostatistics *8*, 118-127.

Josset, L., Belser, J.A., Pantin-Jackwood, M.J., Chang, J.H., Chang, S.T., Belisle, S.E., Tumpey, T.M., and Katze, M.G. (2012). Implication of inflammatory macrophages, nuclear receptors, and interferon regulatory factors in increased virulence of pandemic 2009 H1N1 influenza A virus after host adaptation. J. Virol. *86*, 7192-7206.

Manzanero, S. (2012). Generation of mouse bone marrow-derived macrophages. Methods Mol. Biol. *844*, 177-181.

Sheehan, K.C., Lai, K.S., Dunn, G.P., Bruce, A.T., Diamond, M.S., Heutel, J.D., Dungo-Arthur, C., Carrero, J.A., White, J.M., Hertzog, P.J., *et al.* (2006). Blocking monoclonal antibodies specific for mouse IFN-alpha/beta receptor subunit 1 (IFNAR-1) from mice immunized by in vivo hydrodynamic transfection. J. Interferon Cytokine Res. *26*, 804-819.